Journal of Thermal Analysis, Vol. 47 (1996) 247-258

THERMAL DEGRADATION OF ETHYLENE (VINYL ACETATE)
Kinetic analysis of thermogravimetric data

M. L. Marín[1], A. Jiménez[1], J. López[2] and J. Vilaplana[2]*

[1]Departamento de Química Analítica, Universidad de Alicante, Ap. 99, 03080 Alicante
[2]Instituto Tecnológico del Juguete (AIJU), Av. Industria s/n, 03440 Ibi, Alicante, Spain

Abstract

Ethylene (vinyl acetate), EVA, is a copolymer which is thermally degraded at high temperatures, with acetic acid release at approximately 620 K. This release can be studied by using thermal methods, and in particular thermogravimetric analysis.

The present work was focused on establishing the polymer weight loss with temperature in order to calculate the activation energy of the overall deacetylation process. To obtain the final results, a Mettler TC50 instrument coupled with a Mettler TC11 microprocessor was used.

The activation energies of four different industrial EVA formulations were calculated. The results obtained by applying different kinetic methods reported in the literature agreed reasonably well; they were compared in order to select the best method of reporting EVA deacetylation results.

Keywords: ethylene (vinyl acetate), kinetics, polymer

Introduction

One application of thermal methods of analysis in polymer science is for the determination of kinetic parameters (reaction order, pre-exponential factor and activation energy). Among them, thermogravimetric analysis (TG) is a commonly used technique because of its simplicity and the information afforded from a simple thermogram. For calculation of the above parameters, many methods have been proposed [1–4]. In the present study, we have calculated the activation energy by applying some of those methods to ethylene (vinyl acetate) (EVA), in the same way as proposed for PVC in a previous work [5].

Thermal degradation of EVA

EVA is a copolymer of ethylene and vinyl acetate as a polar group. When EVA is heated and undergoes thermal degradation, the first product evolved is

* Author to whom all correspondence should be addressed.

0368–4466/96/ $ 5.00

John Wiley & Sons, Limited
Chichester

acetic acid (HAc). This deacetylation reaction starts at about 560 K, the maximum reaction rate being observed 30 K higher. This result is probably due to the fact that every short sequence of vinyl acetate (VA) in the copolymer requires its own initiation step, as suggested by McNeill *et al.* [6]. The mechanism of formation of HAc is based on ester pyrolysis, which takes place through a cross-linking mechanism [7] as follows:

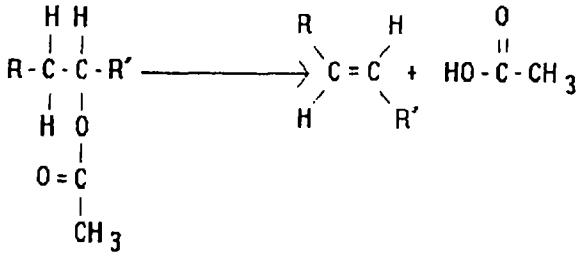

HAc is therefore the main product evolved from EVA in this temperature range. However, small amounts of chain fragments, ketene, carbon monoxide, carbon dioxide and water have also been observed, those probably being formed during the thermal decomposition of the evolved HAc. Additionally, butene and acetaldehyde have been observed.

Sultan and Sörvik [8–10] found by isothermal analysis that the evolution of HAc increases with increasing temperature and VA content. They considered the fast initial release to come from the HAc formed in the samples during processing and storage. On the other hand, Salin and Seferis [11], working under dynamic conditions, found that low heating rates are necessary for good resolution.

The dacetylation process may be catalysed by acids such as HCl, and in some cases by the evolved HAc. Inhibitors of radical reactions do not influence the deacetylation rate.

EVA undergoes a two-stage decomposition, the first stage being HAc evolution, i.e. the loss in mass is proportional to the amount of acetate groups initially present in the system. The second decomposition stage is due to chain scission. In this study, we have focused on the application of kinetic methods to the deacetylation process.

Kinetic methods

The dynamic kinetic methods used in the present study are based on the following equation:

$$d\alpha/(1-\alpha)^n = (A/\beta)\exp(-E_a/RT)dT \quad (1)$$

This is the fundamental expression of analytical methods for calculation of the kinetic parameters on the basis of TG data.

In this study, a first-order reaction was assumed to be applicable for the system and all methods were evaluated by considering first-order kinetics.

We have used three integral methods, based on integration of Eq. (1), to obtain the activation energy of the deacetylation process. One of them was that of Van Krevelen [1], which is based on the following expression:

$$\ln|\ln(1-\alpha)| = \ln[(A/\beta)(0.368/T_m)^{E_a/RT_m}\{1/(E_a/RT_m+1)\}] + \{E_a/RT_m) + 1\}\ln T \quad (2)$$

where α=conversion grade, R=gas constant (8.3136 J mol^{-1} K^{-1}), A=pre-exponential factor (min^{-1}), β=heating rate (K min^{-1}), E_a=apparent activation energy (kJ mol^{-1}) and T_m=temperature of maximum loss in mass (K).

Thus, a plot of $\ln|\ln(1-\alpha)|$ *vs.* $\ln T$ will give straight lines for different heating rates and the activation energy can be calculated.

The method of Horowitz and Metzger [2] is based on a similar equation:

$$\ln|\ln(1-\alpha)| = E_a\theta/RT_s^2 \quad (3)$$

where $\theta=T-T_s$ and T_s is the temperature such that $1-\alpha=1/e$. A plot of $\ln|\ln(1-\alpha|$ *vs.* θ gives a straight line whose slope permits easy determination of the activation energy.

Finally, Coats and Redfern [3] proposed a plot of $\log[(-1/T^2)\ln(1-\alpha)]$ *vs.* $1/T$, the slope being $E_a/2.3R$.

In the Van Krevelen and Horowitz-Metzger methods, an asymptotic expansion of the exponential factor in Eq. (1) is performed before integration; in the Coats and Redfern method, the exponential integral is approximated by an appropriate function.

All of these methods furnish the activation energy from a single TG curve and allow study of the influence of the heating rate upon the activation energy. These methods have been selected because the obtained plots have correlation coefficients near 1. Mass losses caused by deacetylation are smaller that those involved in main chain scission, so differential methods will give lines with a very poor correlation.

On the other hand, the Kissinger method is based upon the derivation of Eq. (1) and it is a 'many curves' method, i.e. it presumes that the activation energy, reaction order and pre-exponential factor do not depend on the heating rate. The Kissinger [4] method utilizes the following expression:

$$-d(\ln\beta/T_m^2)/d(1/T_m) = E/R \quad (4)$$

If we plot $\ln\beta/T_m^2$ *vs.* $1/T_m$, a straight line can be obtained.

Experimental

Apparatus

TG was performed with a Mettler TG50 microbalance coupled with a Mettler TC11 TA microprocessor and controlled by Mettler Graphware TA72 software. This microbalance was calibrated by using the discontinuous change in magnetic properties with temperature of metals such as traphoferm, nickel and isotherm. As the temperature increases, the individual metal samples lose their ferromagnetic properties at well-defined temperatures and they are no longer influenced by the magnet. The Curie point of every metal can be calculated and therefore the microbalance can be calibrated at different heating rates.

Materials

EVA copolymer was supplied in the form of granules by Repsol (Spain). It has a low VA content and properties very similar to those of low-density polyethylene. As the VA concentration increases, the end-product has a lower degree of crystallinity and displays behaviour very similar to that of products such as thermoplastic rubbers or plasticized PVC. The properties of EVA are basically defined by the melt flow index (indirect measurement of the molecular weight) and the VA content. The main properties of these materials are shown in Table 1.

Table 1 Characteristics of materials

Grade	Vinyl acetate/%	Melt flow index/g(10 min)$^{-1}$	Tensile strength at break/MPa	Elongation at break/%	Shore A	Hardness D
PA–533	9	9	11	600	95	40
PA–561	12	0.6	22	700	96	45
PA–538	18	2	21	750	90	38
PA–541	20	3	21	800	91	39

Operating procedure

The EVA degradation process was followed by monitoring the loss in mass with increasing temperature in a controlled N_2 atmosphere (300 ml min^{-1}). Cylindrical alumina crucibles (40 μl) were used and every sample was examined without previous treatment. The sample mass was about 8–10 mg. The temperature range of the experiments was between 30 and 600°C in order to complete decomposition of the polymer, and they were conducted at a constant heating rate.

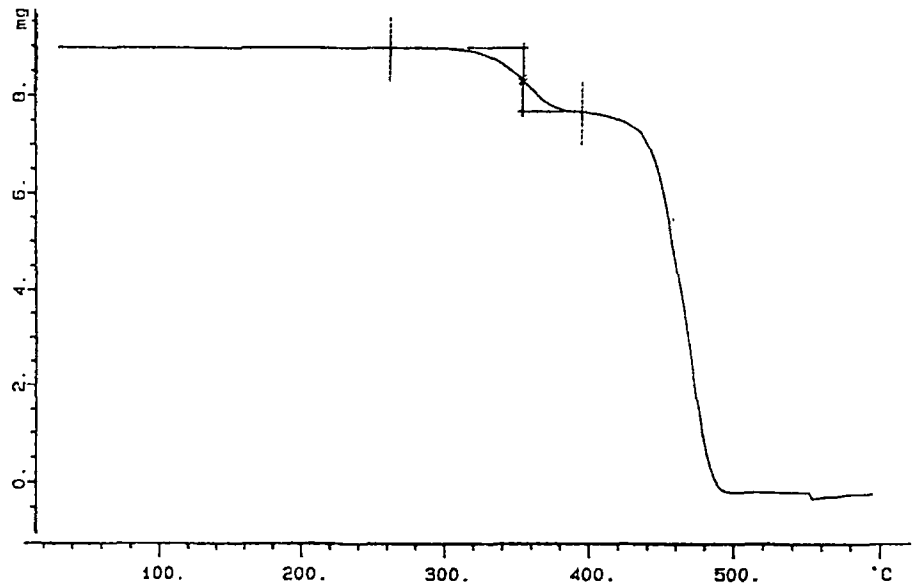

Fig. 1 TG curve for an EVA sample heated in N_2 atmosphere

Results and discussion

A typical thermogravimetric curve is shown in Fig. 1. It will be noted that deacetylation began at 570 K and was finished at 670 K. Air was introduced at 770 K and this change of atmosphere was responsible for the third step in Fig. 1.

The decomposition of EVA depended strongly on the heating rate. The maximum deacetylation temperature increased with increasing heating rate, with a minimum value at 10 K min^{-1}, while there was no relation with the VA content of the samples. Results are shown in Fig. 2.

Table 2 Activation energy (kJ mol^{-1}) calculated by Van Krevelen method

β/K min^{-1}	EVA-9	EVA-12	EVA-18	EVA-20
2	144.17	136.63	160.04	154.77
4	165.91	146.93	167.14	161.37
5	140.22	167.53	168.90	187.69
8	190.88	162.67	166.83	179.05
10	185.12	162.01	182.37	179.72
20	182.08	176.47	200.82	201.85
30	204.76	185.48	196.53	200.35
40	169.74	182.80	164.60	201.10
50	189.61	167.02	208.43	200.75

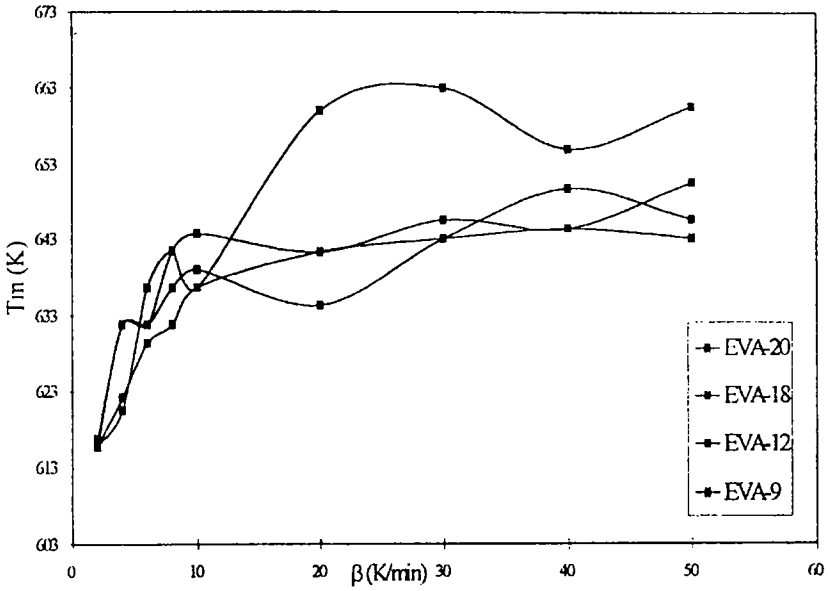

Fig. 2 Maximum deacetylation rate temperature variation with heating rate for different EVA

Application of kinetic methods

The data obtained were analysed by applying the above kinetic methods. Typical plots from the application of these methods are given in Figs 3, 4 and 5. The values found reveal similar behaviour relative to the maximum deacetylation temperature. Results of the application of the methods are given in Tables 2, 3 and 4. It can be observed that there is a dependence on the heating rate.

Table 3 Activation energy (kJ mol^{-1}) calculated by Horowitz and Metzger method

β/K min^{-1}	EVA–9	EVA–12	EVA–18	EVA–20
2	145.71	137.68	161.54	155.15
4	167.99	148.28	168.23	162.46
5	141.21	169.47	171.08	190.10
8	192.33	164.14	168.38	180.88
10	187.01	165.29	183.62	182.16
20	182.24	180.04	204.95	204.21
30	204.74	188.56	199.70	204.21
40	172.25	188.04	165.53	205.62
50	191.14	171.23	213.22	205.52

Table 4 Activation energy (kJ mol^{-1}) calculated by Coats and Redfern method

β/K min^{-1}	EVA–9	EVA–12	EVA–18	EVA–20
2	137.43	129.66	152.76	146.47
4	158.69	138.63	163.30	153.15
5	132.59	159.11	161.39	179.45
8	182.00	154.80	157.90	170.75
10	176.83	154.35	173.50	171.71
20	174.41	169.89	195.94	192.88
30	195.15	178.36	189.70	192.77
40	160.10	176.55	156.59	193.83
50	179.69	159.58	201.75	193.63

The activation energy values obtained by means of the Van Krevelen and Horowitz-Metzger methods are very close. This is absolutely normal since both methods are based on an approximation of $[\exp\{-E_a/RT\}]$ before integration. The Coats-Redfern method gives slightly smaller values, but these are more correct since this method uses a rather good approximation of the exponential integral.

In order to clarify the influence of β, mean values of E_a for different heating rates (Van Krevelen, Horowitz-Metzger and Coats-Redfern methods) are plot-

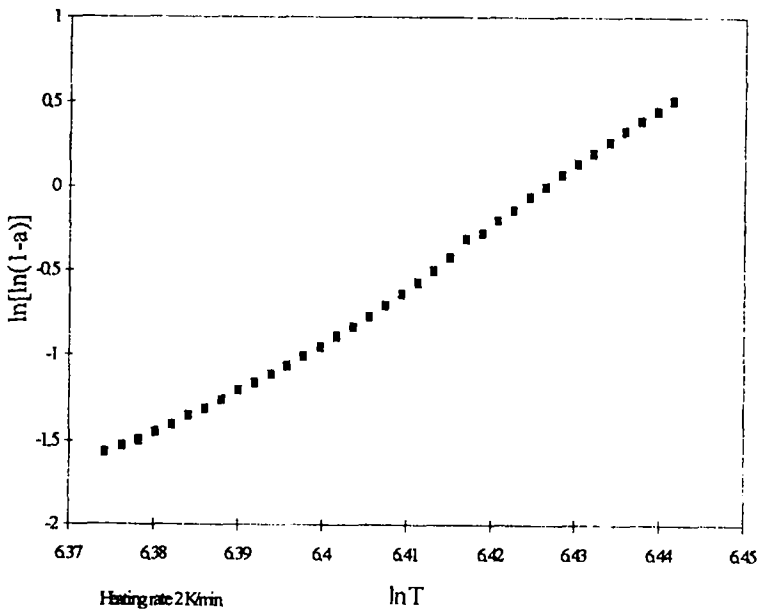

Fig. 3 Van Krevelen method applied to experimental data

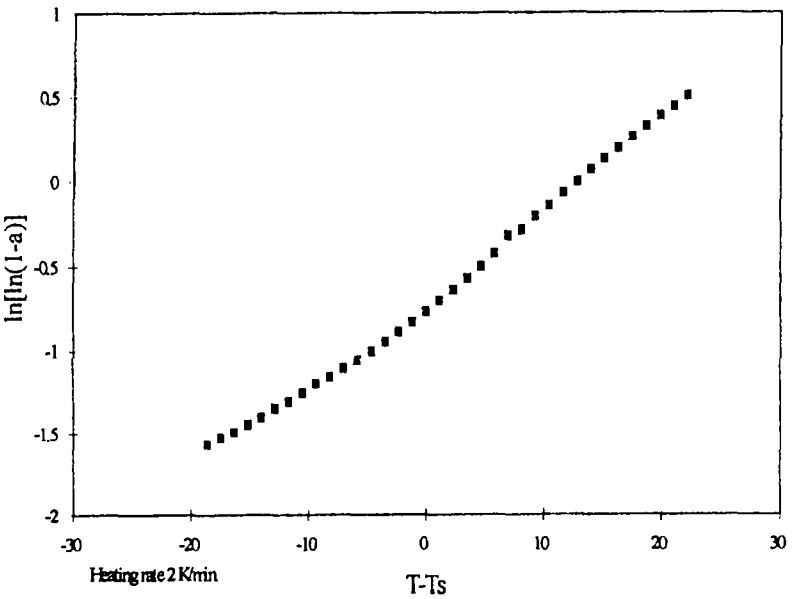

Fig. 4 Horowitz and Metzger method applied to experimental data

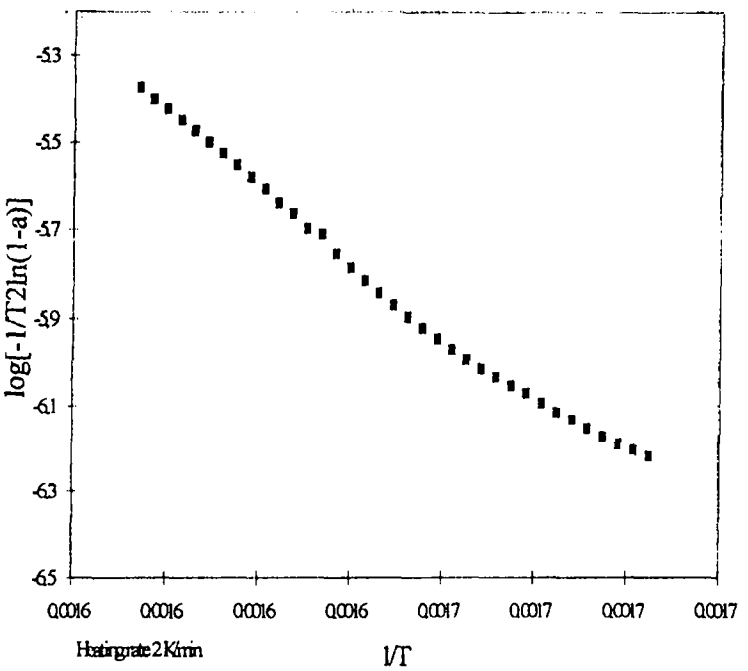

Fig. 5 Coats and Redfern method applied to experimental data

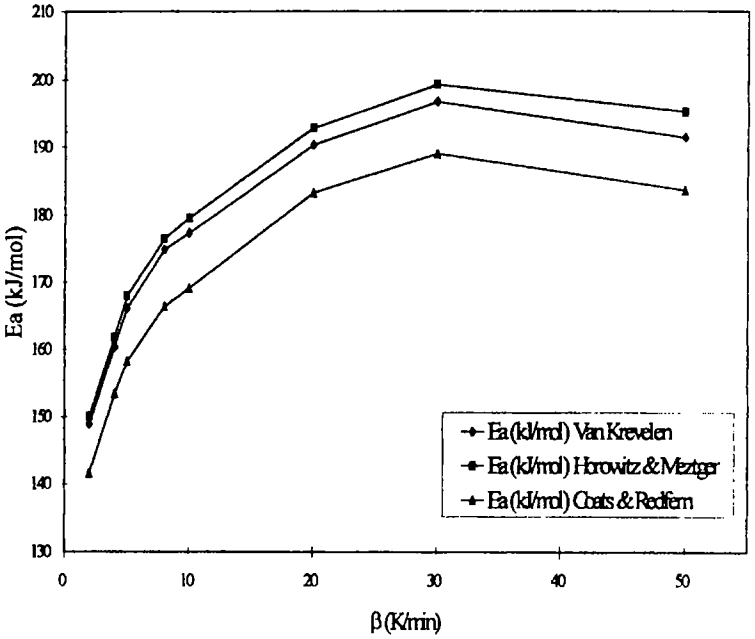

Fig. 6 Mean values of E_a for different heating rates

ted in Fig. 6. On increase of β, the mean E_a value increases up to $\beta=20$ K min^{-1}, and from this value on it remains practically constant (182±6 kJ mol^{-1}). These results are valid only for the indicated sample mass and gas flow.

Table 5 Slopes of E_a *vs.* β plots

Method	EVA–9	EVA–12	EVA–18	EVA–20
Van Krevelen	0.64	0.59	0.64	0.80
Horowitz-Metzger	0.64	0.66	0.69	0.88
Coats-Redfern	0.58	0.62	0.64	0.83

The influence of β upon the activation energy for each material can be judged by performing a linear regression for the E_a *vs.* % VA dependence, as can be observed in Table 5. The slopes of the E_a *vs.* β plots are indicated in Table 5. From these results, it can be concluded that E_a becomes more sensitive to β with increasing VA content.

The values obtained by using these methods are similar, but there are differences in the results when we apply the Kissinger method because the activation energy is calculated with the heating rate variation related to the maximum deacetylation temperature. Results of the application of this method are given in

Tables 6 and 7. It can be noted that differences between the E_a values obtained by means of the Kissinger method and the single curve methods are higher.

Table 6 Summary of activation energy (kJ mol^{-1}) results for thermal deacetylation of EVA

Method	EVA–9	EVA–12	EVA–18	EVA–20
Van Krevelen	175±22	165±16	179±18	185±18
Horowitz-Metzger	176±21	168±17	182±19	188±19
Coats-Redfern	166±21	158±16	173±19	177±18

Table 7 Activation energy (kJ mol^{-1}) calculated by Kissinger method

EVA–9	EVA–12	EVA–18	EVA–20
184.29	301.92	313.98	334.98

With regard to the catalytic effect of HAc, the results obtained seem to be consistent with such an effect. Since E_a values derived from TG curves do not mean real activation energies, in the case of a catalytic effect E_a need not decrease with increasing VA content. Generally, in TG kinetics, with increasing β the derived E_a values decrease [12, 13]. This is probably due to the fact that, with increasing β, the role of the diffusion of gaseous products becomes more important; their departure from the sample is hindered, and the loss in mass becomes slower, which in terms of kinetic parameters means decreasing E_a and A values. In the case of EVA, exactly the opposite effect is observed, i.e. E_a increases with increasing β. This might be due to the catalytic effect of HAc. With increasing β, the diffusion is hindered and increasing local HAc concentrations may be expected, which in the case of a catalytic effect increases the pyrolysis rate and consequently E_a.

Conclusions

In thermal analysis, the heating rate influences the results because of the relationship between the apparatus response and the reactions that occur in the sample. This behaviour could be caused by the difference between the temperature of the furnace and that of the sample at high heating rates. To ensure that the sample temperature is adjusted to the programme in a dynamic measurement, the furnace temperature must be higher to a certain degree. This temperature difference depends on the temperature equilibration function and on the heating rate. The furnace temperature advance can be calculated according to the following equation:

$$\Delta T = T_{\text{furnace}} - T_{\text{sample}} = \tau \, dT/dt \tag{4}$$

where τ is a time function.

It can be considered that it is necessary to reach a fixed temperature T_i (T_{sample}) to obtain a definite response of the sample, and Δt would be the time to transmit the final temperature to the whole sample. Therefore, the measured temperature should be:

$$T_r = T_i + \beta\Delta t(\beta) \tag{5}$$

Δt depends on the sample nature, geometry, temperature and heating rate.

Melling *et al.* [14] indicated a relationship between temperature differences and time range for DTA, considering the sample as a sphere where every volume element is separated from the centre of the sample by a length r. The heat balance equation for the centre element can be considered as:

$$[4k_{1/2}(T_2 - T_1)\Delta t]/\rho_1 C_1(\Delta r_s)^2] + H\Delta t/\rho_1 C_1 - J(T_1 - T_o)\Delta t + T_1 = T_1' \tag{6}$$

where

$$k_{1/2} = 1/2[(k_f - k_s)(x_1 - x_2)] + k_s \quad \text{with} \quad k_f = k_r(1 + aT + bT^2) \tag{7}$$

k_r = conductivity of product at ambient temperature,

$$k_s = k_o(1 + cT + dT^2) \tag{8}$$

k_o = conductivity of starting material at ambient temperature,
a, b, c and d = constant,
x_n = molar fraction of products formed in the nth element,
T_n = temperature of nth element,
T_o = room temperature,
Δt = small time step,
ρ_n = density of nth element,
C_n = specif heat of nth element,
Δr_s = radius of sample/number of elements,
H = internal heat generation per unit volume and unit time,
J = heat transfer coefficient of heat loss along centre thermocouple, and
T_n' = temperature of nth element after time Δt.

If we use this relationship, J is not applicable because the thermocouple has not been used. Hence

$$\Delta t = (T_1' - T_1)/[K_1(T_2 - T_1) + K_2] \tag{9}$$

where

$$K_1 = 4k_{1/2}/\rho_1 C_1(\Delta r_s)^2 \tag{10}$$

The influence of β on $T_1'-T_1$ is difficult to evaluate because there are temperature differences in the sample. T_2-T_1 represents the temperature difference between the sample centre and an external ring. Thus, if we extrapolate, we can consider T_2 to be the sample external temperature (proportional to β). From Eq. (9), we can get

$$\Delta t(\beta) = a/(\beta b + c) \tag{12}$$

where

$$a = T_1'-T_1 \tag{13}$$

$$K_1(T_2 - T_1) = \beta b \quad \text{and} \tag{14}$$

$$K_2 = c \tag{15}$$

From Eq. (5):

$$T_r = T_{sample} + a\beta/(b + c\beta) \tag{16}$$

From Eq. (16), it can be concluded that there is a dependence between T_r and β for low β values, a constant being obtained when β is high enough.

Considering that E_a is proportional to T_r, an equation similar to Eq. (16) can be obtained:

$$E_a(\beta) = E_o + a\beta/(b + c\beta) \tag{17}$$

This equation is consistent with the experimental data.

* * *

The authors wish to express their appreciation to DGICYT (Spain), Project AMB 94-107, for financial support of this study.

References

1 D. W. Van Krevelen, C. Van Heerden and F. J. Hutjens, Fuel, 30 (1951) 253.
2 H. H. Horowitz and G. Metzger, Anal. Chem., 35 (1963) 1464.
3 A. W. Coats and J. P. Redfern, J. Polym. Sci., 3 (1965) 917.
4 H. E. Kissinger, Anal. Chem., 29 (1957) 1702.
5 A. Jiménez, V. Berenguer, J. López and A. Sánchez, J. App. Polym. Sci., 50 (1993) 1565.
6 I. C. Mc Neill, A. Jamieson, D. J. Toshand and J. J. Mc Clune, Eur. Polym. J., 12 (1976) 305.
7 J. Kaczaj and R. Trickey, Anal. Chem., 41 (1969) 1511.
8 B. Ake-Sultan and E. Sörvik, J. App. Polym. Sci., 43 (1991) 1737.
9 B. Ake-Sultan and E. Sörvik, J. App. Polym. Sci., 43 (1991) 1747.
10 B. Ake-Sultan and E. Sörvik, J. App. Polym. Sci., 43 (1991) 1761.
11 I. M. Salin and J. C. Seferis, J. App. Polym. Sci., 47 (1993) 847.
12 J. Zsakó et al. J. Thermal Anal., 17 (1979) 123.
13 J. Zsakó et al. Thermochim. Acta, 45 (1981) 11.
14 R. Melling, F. W. Wilburn and R. M. McIntosh, Anal. Chem., 41 (1969) 1275.